

Measure of ground deformations by SAR Interferometry in Tangier city (Northern Morocco)

I. El medrai¹, T. Mourabit², A. Tahayt³

¹Geology Department , Faculty Of Science And Technology, Abdelmalek Essaâdi University, Ziaten B.P. 416 Tangier, Morocco.

²Faculty Of Science And Technology, Mohammed I University, Ajdir B.P. 34 Al-Hoceima, Morocco.

³Department Of Earth Sciences, Scientific Institute, Mohammed V University Of Rabat. B.P. 703, Rabat, Morocco.

Abstract: This study presents the deformations of earth's surface in Tangiers (Northern Morocco). The follow-up of these deformations was made by the Interferometric Synthetic Aperture Radar technique (InSAR). The application of InSAR in an urban environment allows to obtain a spatial distribution of the ground deformation within subcentimeter resolution. The InSAR time series analysis methods give an accurate estimation of the deformation rates.

In this work we use ROI-PAC software to generate the interferograms from images acquired by Envisat between 2003 and 2010. In order to calculate the deformation rates (on the line of sight) by time series analysis we applied pi-rate software. The stacking map shows major uplift up to 20 mm/year in the coastal and southern zone of Tangier, and subsidence of the soil that can reach 15mm/year in some areas.

To evaluate these results, we used the interferometric coherence as a measurement of the reliability of the interferometric phase. We calculated also the error map. All the deformation areas present a very high coherence and the associated error is almost negligible, also the atmospheric noise level is reduced during time series analysis.

We suggest that the origin of these deformations (uplifts and subsidence) can be explained by the mechanical behavior of the soil combined with the tectonic movements.

Keywords: InSAR, stacking map, deformation, mechanical behavior, tectonic.

I. INTRODUCTION

Tangier is located at the junction of two seas at the far north of Morocco, on a tectonic convergence zone between the African and Eurasian plates. This area is home of active tectonics highlighted by geological and seismological studies (1) (2).

The study area is located in the external Rif domain. In particular the intrarif units (mainly composed of Mesozoic land of the Triassic in the average Cretaceous) and the flysch nappes (3) (4) . They are mainly anticlinorium with synmetamorphic structures of Miocene age (5) (6) (7).

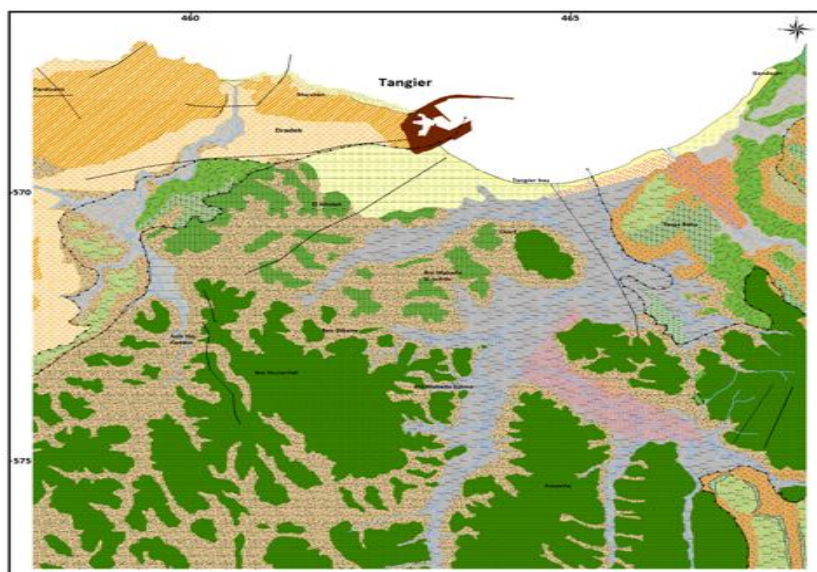




Fig 1: Geotechnical map of Tangier (simplified and modified from the Geotechnical Map of Tangier, 1:25 000)

Figure 1 shows that the area is covered by a set of nappes (Numidian, Bni Ider and Tisirene). These flysch nappes (Series going from the Cretaceous to the lower Miocene) are expelled in the form of thrust sheets on their para-autochthon unity of Tangier starting at the upper-middle Burdigalian. (8) (9)

The majority of the terrain in our study area are well represented by the nappe of Numidian flysch. These Numidian flysch terrains forms clearly marked crests, and armed with many sandstone beds of lower Oligocene to Miocene, and are juxtaposed on the hills in Cretaceous substratum of Tangier unit and on Melloussa nappe (10) (11) .

The terrain of Numidian flyschs is following the establishment of massylien flysch (12) (13). They will then be detached from its substratum in Burdigalian, the end of their establishment dating from the Tortonian. (14) (9)

From this general scenario, we can conclude that the tectonic activity of the region was, from the late Miocene, comparatively less than during the Palaeogene and the early-middle Miocene, although many deformations affected this region from the Tortonian (late Miocene) onwards. (15)

As for the geotechnical characteristics, we can divide the materials into four large units of soil: The clay soils, the sandstone soils, the marly soils and the sandy soils.

The clay rock is observed on the clay hilltops and on their upstream catchment. The argillites and the marls (very plastic), are quite rare even in the depth due to the mechanical and structural forces in relation with the tectonic. Those forces are sometimes profoundly folded or even crushed the claystone mother. (16)

Sandstones have a restricted extension, they form small isolated outcrops, arranged by turbiditic and flexo-turbiditic rhythms with thin clay beds (7), and they are distinguished on the landscape with a particular morphology. Even with their reduced extension, they give an exceptional structure and a high importance on the clays and the argillites, and form with the limestone-marl series the resistant areas.

The limestone-marl series are rare and with poor quality and reduced area (Msakhoch and Tanja Balia), limestones are rather thin, as benches from 5 to 10 cm, sometimes 20 cm and are a significant heterogeneity in structure. The marly and argillaceous past are abundant. (11)

The sand dunes have been invaded by the constructions. They generally may passed under the concrete or under the back filling materials (17). Those dunes fill the small depressions, and they present a poor compactness.

With this position on the both seaboard, it has known in these last decades a significant development of commercial, industrial and administrative activities. This has led to rapid development of urbanization and the expansion of facilities to sites less favorable.

This makes it necessary a careful study to determine the behavior of the land in order to limit the human damage through prevention and preparation.

In order to assess geological risks in this region, we used InSAR time series analysis method to measure the ground displacement rates.

II. METHODOLOGY

Radar interferometry is a technique based on the use of two radar images of the same area, acquired with a slightly different angle of incidence, at the same time or at two different times (18). To detect changes in the surface of the earth, these two images are to be taken more or less from the same position in space, but on two different dates in order.

The principle of InSAR is to compare the phases of two radar images with the objective of obtaining a map of changes in the distance between the radar antenna and the studied object.

The InSAR allows mapping the displacement of large areas with high resolution (in the order of centimeters to tens of meters) without requiring ground instrumentation on the study area. These characteristics have allowed for better monitoring and better modeling of various processes. They can be located in difficult access zones, or weakly equipped in GPS stations and other processes generating very small deformation such as the urban subsidence of Paris are also monitored by InSAR (19). Furthermore, the InSAR data can be combined with other types of data (GPS, seismic) to constrain models, that's what Tahayt & al (2009) did for the earthquake Alhociema 2004 (20), and Delouis & al (2010) for the earthquake of February 27, 2010 in Chile (21).

The generation of the differential interferograms has to pass through several steps going from the selection of the radar data, the generation of Digital Elevation Model DTM and topographic map until the application of ROI-PAC generator program of interferometric images, and then to measure of the ground displacement by π -rate (22).

A. Selection of satellite images

The choice of satellite images is based on two essential parameters:

The Baseline: To reduce the noise of geometric decorrelation due to the baseline, We chose, as constraint, to have a small baseline (in meter) in the range of [-150, 150].

The date offset: This criterion of choice may be long or short. Indeed, on the one hand, we should rather choose small differences for having interferograms less noisy and reduce noise of temporal decorrelation, and on the other hand, a long date offset in order for significant changes can take place between acquisitions. (23) The Interferometric couples with these constraints are generated, and thereafter, processed with ROI-PAC software (24). (Figure 2)

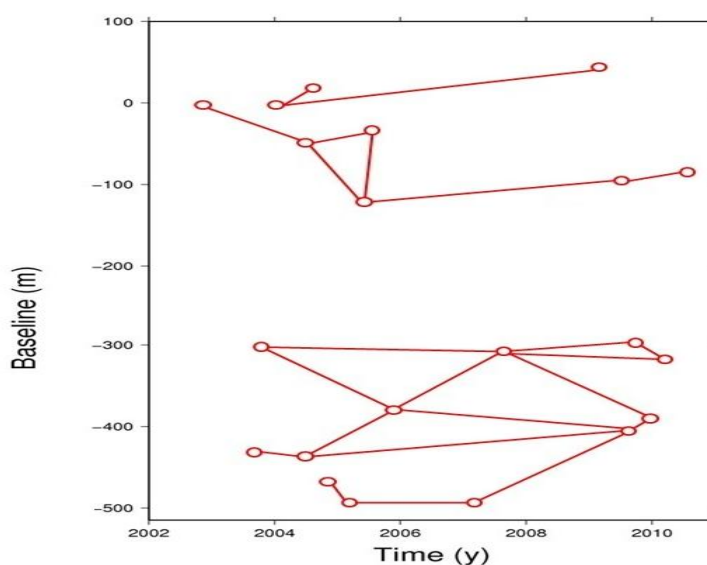


Fig 2: Temporal distribution of interferometric couples with constraints (Baseline = [-150, 150] m, Date offset = [0, 2500] days)

B. Data processing

The ROI -PAC provides tools to calculate the correlation between two SAR images (25), to generate the displacement maps it uses RAW images and telemetry data in combination with a DEM of the imaged scene (26). In the chain D- InSAR proposed by ROI-PAC, the DEM operates at three levels: orbital corrections, compensation of topographic fringes and georeferencing the outputs of processing (coherence, developed phase or amplitude). (27)

Once the data introduced, the "ROI-PAC" software will be ready to generate the interferometric products by executing a set of tasks simultaneously. Starting by the image registration (matching two SLC's pictures), after that the re-sampling of the slave image. If this one have not the same size as the master image (the master image is, by default, the first one selected) in order to make that pictures perfectly supposable, passes by the calculation of the products (In radar geometry), the orbital and topographic correction and until the filtering the results. (Figure 3)

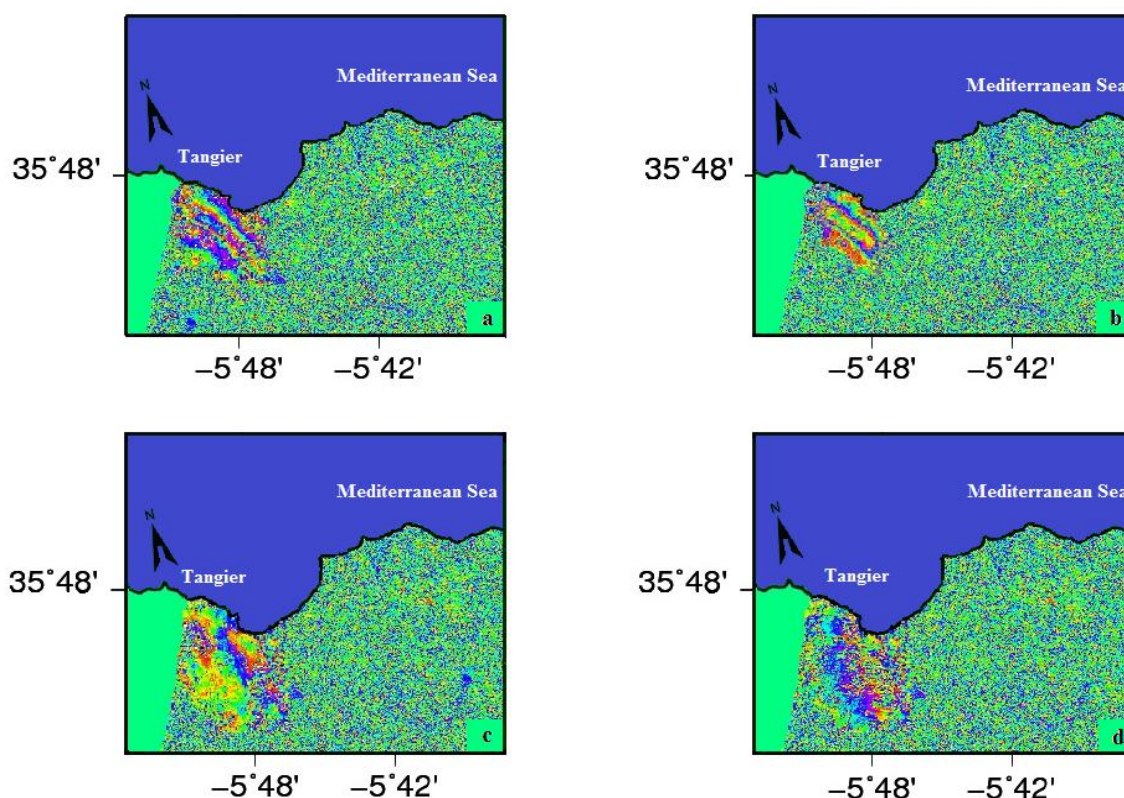


Fig 3: Differential interferograms geocoded filtered and used for the detection of the deformation in the ground.

- a) Combination of images 09/06/2004 and 03/02/2010
- b) Combination of images 14/07/2004 and 03/08/2005
- c) Combination of images 12/09/2007 and 14/04/2010
- d) Combination of images 12/08/2009 and 01/09/2010

The "ROI-PAC" software uses a nonlinear spectral adaptive algorithm filtering based on the spatial analysis of the change of frequency of fringes, to filter the noise of decorrelation geometrical and temporal and to clarify the fringes (those we are interested in our work) due to field displacement (28). This treatment step is based on the coherence (areas not affected by the noise of decorrelation), and aim to extract the most coherent areas to propagate them on the neighborhood and improve the phase. Then, it transposes the image produced from the radar geometry to the ground geometry given by the DEM.

The image produced forms the "interferogram", result of treatment by ROI-PAC. We masked all zones outside the area of interest. We developed a script under MATLAB based on the generated DEM. This script defines the surface of the unused pixels.

To eliminate the maximum of disturbances (noise) and so improve the legibility of interferograms and to quantify the movement, we used the π -rate software.

π -rate is a software based on Matlab that estimates the rate of displacement, the time series and their uncertainties associated from a set of InSAR images. It comes from the multi-interferogram method (29) (30).

In order to reduce the atmospheric noise we built (under π -rate) an interferogram representing the total displacement by stacking four interferograms which already showing low amplitude atmospheric artifacts.

The stacking allow strengthening the signal to noise ratio, which aims to make a series of interferograms having a maximum coherence between interferometric couples (31) (32) (33) (34) (35) .This stacking is valid only for the deformations that not showing significant changes over time (36) .

This method based on averaging multiple interferograms (37) (38). When using N interferograms, the noise will be reduced by a factor of \sqrt{N} , however we can use the stacking only if all interferograms are independent (an image can only be used once) and it should not exist any correlation between artifacts and topography (39). It may be possible that some images are excluded by this selection. The purpose of this method is to get a temporal tracking of movements; the reference of a deformation will be the oldest date.

The selected Interferometric couples for stacking are those who have seemed to us the most interesting in terms of quality (low noise, high degree of coherence, low atmospheric component) and possibilities of interpretation for deformation tracking (periods covered) (40).

To check the interferometric coherence of the image result from stacking. We need to check, each interferogram and the behavior of each pixel compared to its neighbors.

The coherence map indicates areas in which we observe coherent pixels at almost all of the interferograms, by averaging between the different image of standard deviation we get the location of the coherent pixels. Those pixels are whose average standard deviation is very low in time. The coherence is used as a measurement of reliability of the interferometric phase . (41)

To complete the evaluation of results, we also calculated the errors produced to compare with the original information. With the map of error, we can get an idea about the accuracy of the deformation. A low error will become a high confidence (42):

$$\text{Confidence [i][j]} = \frac{1}{1+\text{Error [i][j]}}$$

III. RESULTS AND DISCUSSION

The comparison between many independent interferograms, allows to reject the possibility that the signature could due to the atmospheric artifacts. In fact, this is repeated identically from an acquisition to the other one. The presence of a stable signature on many interferograms, confirms the detection of the soil deformation.

Given that, the phase signal of the obtained from an interferometric couple present many characteristics. Which makes it difficult to exploit, and to improve the clarity of the fringes (increase the link between the atmospheric components of the phase and those of the deformation) and quantify the movement. We built an interferogram by making the sum of four interferograms that's cover the entire period going of June 2004 at September 2010 ; reducing the influence of the residual atmospheric structures of a factor $\sqrt{4}$. (Figure 4)

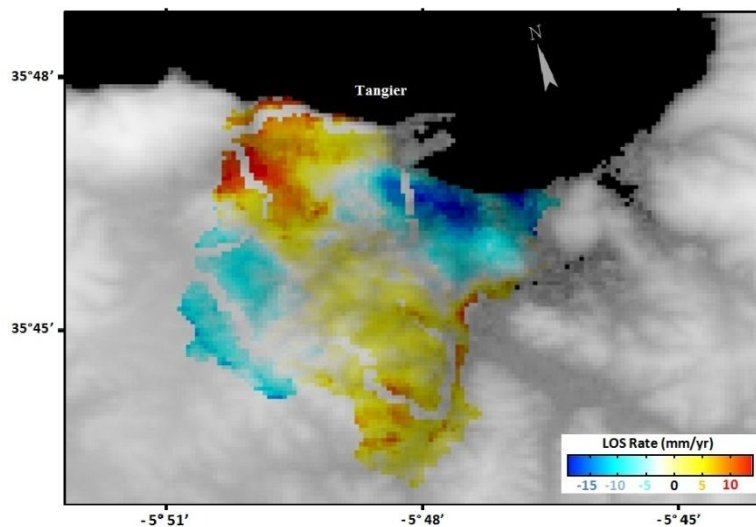


Fig 4 : Stacking map ; The Sum of four interferograms, 09/06/2004 - 03/02/2010, 14/07/2004 - 03/08/2005, 12/09/2007 - 14/04/2010, and 12/08/2009 - 01/09/2010.

The result in figure 4 gives an estimation of the deformation rates between 2004 and 2010. This deformation present a maximum uplift of 20 mm/year, and a maximum of subsidence of the soil of 15mm/year in some areas.

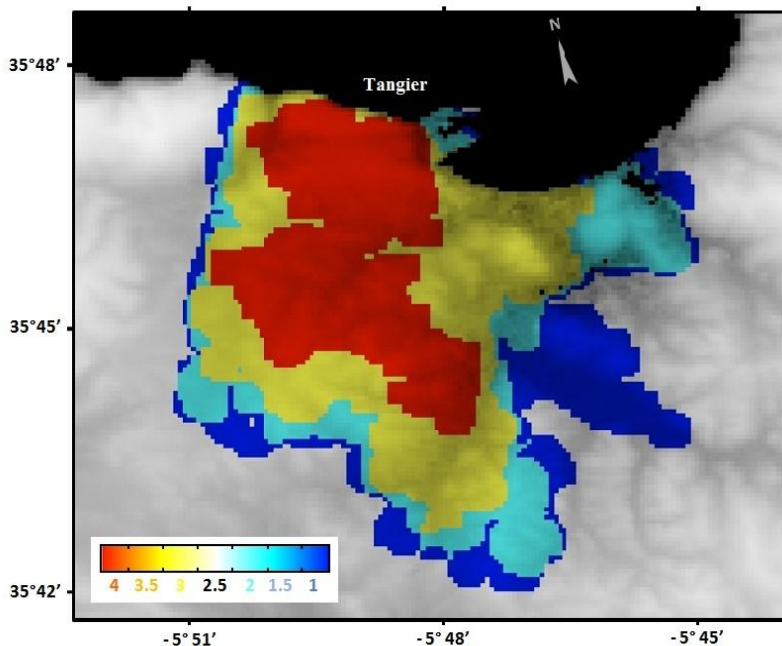


Fig 5: Map of coherence based on the behavior of each pixel compared to its neighbors, allowing the indication of areas in which we observe coherent pixels at almost all of the interferograms

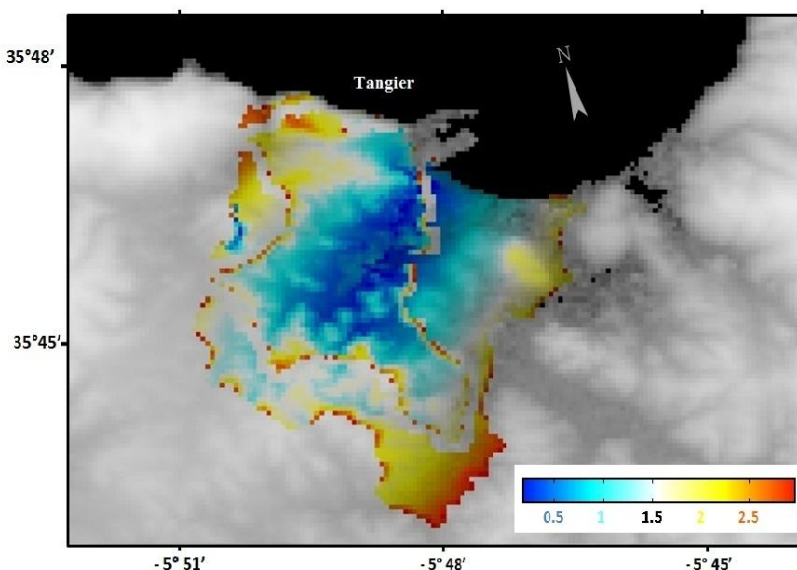


Fig 6: Map of errors. The associated error is almost negligible (between 0 and 0,5 mm). The most marked errors (≈ 2 at 2,5 mm) are on the borders where we have no significant deformation

All the zones corresponding to a deformation present a very high coherence (Figure 5).

The coherence map has allowed us to identify the areas where the variation of phases between the acquisitions are correlated. So it defines the potential quality of the used interferometric couples. Otherwise, the used couples present an information about the reliable phase, then the map of the stacked could be considered as valid.

In the errors map, we can better see most of points are around zero error, that's means that the associate error is almost negligible (between 0 and 0,5 mm). It should be noted that the most marked errors (≈ 2 at 2,5 mm) are on the borders where we have no significant deformation. It can be related to the border effect. (Figure 6)

The origin of these deformations (uplift and subsidence) can be explained by the mechanical behavior of the soil combined with the tectonic movements.

The Tangier unit presents folds of the second phase of folding and a few penetrative schistosity. Therewith, the faults that have played a significant role in the recent tectonic evolution. The instability of the substratum of Tangier unit was active during the entire Neogene period through faults, rockslides and discontinuities (43). The geology of the hinterland is characterized by piling of four flysch nappes which rely on Tangier unit as major abnormal contacts: Melloussa, Beni-Ider, Tisirene and Numidian nappes (44) (45) (46) (47).

The Tangier region is characterized by a humid climate and fast abundant precipitation in winter and autumn. The rains act on the reliefs composed from Argillaceous Sandstone series or argillaceous limestone in where the whole is plastic (83%) except sand of the bay of Tangier where the plasticity is unmeasurable. The hydration of these clays causes their swelling and gives them a high plasticity ; the overhead of the volumes of water trapped in the soil porosity can lead to landslides. The plastic materials behave differently in uppermost parts and in slopes and in the valleys. (48)

The dunes sand filled the small depressions. They have an uniform and very tight granulometry, although sometimes containing a few scattered inclusions of clay nodules, which have a swelling potential talent. Figure 4 provides an estimation of an uplift from 10 to 20 mm / year. This uplift can be explained by the swelling of materials, and significant offsets of Tangier fault, which shows a parallel direction N135 to the Malabata fault. This fault from Alpine age was reactivated normal fault during the Quaternary (49).

In the hills (Marshan, Dradeb, Elmaleh ..) and some plateaus (Bni Makada, Aouama ..), some clay or marly levels (not exceeding a few meters) separate the layers of sandstone bench. Their residual resistance, which have a small fraction of the maximum primary resistance makes the soil highly compressible (≈ 10 to 15 mm/year de of settling) for pressures that exceed the consolidation pressure 1kg/cm^2 . (16)

Downstream of these hills and plateaus, the alluvial deposits and colluvium severely affect the mechanical behavior of the corresponding land. The resistant benches weighs on the soft and the plastics series with great finesse and having a high plasticity index. Their consistency is firm enough at the surface on the first two meters due to the over-consolidation brought by desiccation. These resistant benches produce subsidence up to 5 to 10 mm / year (Figure 4), and the tectonics creates privileged areas for action of erosion by dislocating the materials or creating zones of weakness along fractures or faults, which directly affects the instability of slopes.

The marly schistose present a more clearly schistose aspect with strata very clearly marked but can also be perturbed by the tectonic movements or old landslides. They undergo subsidence in Bni Makada Kdima and Ben Dibane, and uplift in Bni Ouriarhel, Azib Haj Kaddor And the hill of Charf. Their anisotropy is so much more pronounced than in the case of argillites and the dispersions of mechanical properties is much more important. (11)

IV. CONCLUSION

This study emphasized the importance of the InSAR in urban environment. The deep analysis of the interferograms treated by ROI-PAC and π -rate confirms that the fringes are due to the movements of the terrain in the urban area of Tangier. Thoses displacements present an important subsidence up to 15mm/year and an uplift from 20 mm/year in some areas, whose origins can be explained by the mechanical behavior of the soil combined with the tectonic movements.

Indeed, these deformations may lead after construction to a disorder of expansion. This detection is an essential parameter for development and risk management (collapses). The construction projects should be, therefore, the subject for careful geotechnical study to control the risks of instability.

ACKNOWLEDGMENTS

We gratefully acknowledge the gracious hospitality and the generous assistance received from Dr Pierre BRIOLE, Director of Geosciences Department of ENS in Paris, and from Dr Alexis RIGO, Director of the UMR5277 in the Observatoire Midi-Pyrénées in Toulouse.

We also wish to acknowledge the valuable assistance we received from Mr Panagiotis ILIAS and Mr Michel PEYRET.

REFERENCES

- [1]. Vernant, P. Fadil, A. Mourabit, T. and al. Geodetic constraints on active tectonics of the Western Mediterranean: implications for the kinematics and dynamics of the Nubia-Eurasia plate boundary. *J. Geodyn.* 2010. pp. 123-129. Vol. 49.
- [2]. Cherkaoui, T-E. and El Hassani, A. Seismicity and Seismic Hazard in Morocco 1901-2010. *Bull. Inst Sci. Rabat, sec. Sci. Terre.* 2012. Vol. 34.

- [3]. Lespinasse, P. Géologie des zones externes et des flyschs entre Chaouen et zoumi (Centre de la chaîne rifaine, Maroc). PhD thesis, Toulouse. 1975.
- [4]. Chalouan, A. La tectonique de la chaîne de rif -VI- Reunion anual de la comision de tectonica de la S.G.E. Tetouan- Chefchaouen - Fez: 13 a 15 de septiembere 1994. 1994.
- [5]. Andrieux, J. La structure du Rif central. Etude des relations entre la tectonique de compression et les nappes de glissement dans un tronçon de la chaîne alpine. Notes Mém. Serv. Géol. Maroc. p. 235. Vol. 222 bis.
- [6]. Durand-Delga, M. Fontbote, J-M. Le cadre structural de la méditerranée occidentale: in :géologie des chaînes alpines issues de la Téthys. 26 ème Congr. Géol. Fr. Mém. B.R.G.M, 1980. pp. 67- 85.
- [7]. Pique, A. Soulaïmani, A. Laville, E. and al. Géologie du Maroc. 2006. pp. 18- 19.
- [8]. Durand-Delga, M. Hottinger, L. Marçais, J. and al. Données actuelles sur la structure du Rif. Mém. h. sér. Soc. géol. Fr, 1962. pp. 399- 422.
- [9]. EL Kadiri, K. El Kadiri, K-E. Rahouti, A. Oligocène inférieur de la série maurétanienne (nappe des Béni Ider, Rif septentrional, Maroc): implications paléogéographiques. Bull. Inst Sci. Rabat, sec. Sci. Terre. 2003. pp. 73-91. Vol. 25.
- [10]. Chalouan, A. Galindo-Zaldivar, J. Bargach, K. and al. Deformaciones recientes en el frente de la Cordillera Rifeña (Prerif, Marruecos). Geogaceta, 2000. pp. 43-46. Vol. 29.
- [11]. Aboumaria, K. Les formations littorales quaternaire de la péninsule de Tanger (Maroc nord occidental): lithostratigraphie, processus sédimentologiques, pétrologie et corrélations à l'échelle de la Méditerranée centre-occidentale. PhD thesis. Univ Mohammed V - Rabat. 2011. pp. 17-34.
- [12]. Durand- Delga, M. Mattauer, G. Sur l'origine ultra-rifaine de certaines nappes du Rif septentrional. C.R. Somm .Soc. Géol. F. 1960. pp. 22-23. Vol. 2.
- [13]. Blinda, M. Pollution tellurique du littoral nord-ouest du Maroc entre Tanger et Tétouan : Caractérisation, Impact sur l'Environnement et Proposition de Solutions. PhD thesis. Univ Mohammed V - Rabat, 2007.
- [14]. Bouillin, J-P. Le "bassin maghrébin": une ancienne limite entre l'Europe et l'Afrique à l'Ouest des Alpes. Bull. Soc. géol. France, 1986. pp. 547-558. 8. Vol 4
- [15]. El Kadiri, K. De Galdeano, C-S. Pedrera, A. and al. Eustatic and tectonic controls on Quaternary Ras Leona marine terraces (Strait of Gibraltar, northern Morocco).Quaternary Research. 2010. pp. 277-288. Vol. 74.
- [16]. Humbert, M. Mariotti, M-V. Mémoire explicatif de la carte géotechnique de Tanger 1/25 000. Etude géotechnique. Notes Mém. Serv. Géol. Maroc. 1971. pp. 61-99. 222 bis.
- [17]. Oueslati, A. La "Grande dune de Tanger" (littoral du Maroc septentrional): un exemple de disparition d'une entité naturelle d'intérêt paysager et environnemental. 2014. pp. 251-272.
- [18]. Pathier, E. Apports de l'interférométrie radar différentielle à l'étude de la tectonique active de Taiwan. PhD thesis. Univ Paris Est Marne-la-Vallée. 2003.
- [19]. Fruneau, B. Sarti, F. Detection of ground subsidence in the city of Paris using radar interferometry: Isolation of deformation from atmospheric artifacts using correlation. Geophysical Research Letters. 2000. pp. 3981-3984. Vol. 27.
- [20]. Tahayt, A. Feigl, K-l. Mourabit, T. and al. The Al Hoceima (Morocco) earthquake of 24 February 2004, analysis and interpretation of data from ENVISAT ASAR and SPOT5 validated by ground-based observations. Remote Sensing of Environment. 2009. pp. 306-316. Vol. 113.
- [21]. Delouis, B. Nocquet, J-M. Vallée, M. Slip distribution of the February 27, 2010 Mw = 8.8 Maule Earthquake, central Chile, from static and high-rate GPS, InSAR, and broadband teleseismic data. Geophysical Research Letters. 2010. Vol. 37. L17305.
- [22]. Wang, H. Biggs, J. Wright, T.J. π -RATE (v3.1) Poly-Interferogram Rate and Time-series Estimator. <http://homepages.see.leeds.ac.uk/~earhw/resources/others/pirate.pdf>. 2012.
- [23]. Chaabouni, A. Génération et analyse des images interférométriques pour la mesure des déformations de terrain. Project of Study End of Engineers in telecommunication - Sup' Com - Tunis. 2012. pp. 34- 35.
- [24]. Pritchard, M-E, and contributors to the ROI_PAC wiki. Open-source software for geodetic imaging: ROI_PAC for InSAR and pixel tracking. http://www.geo.cornell.edu/eas/PeoplePlaces/Faculty/matt/pub/winsar/InSAR_textbook_for_web_2014.pdf. 2014.
- [25]. Yajing, Y. Fusion de mesures de déplacement issues d'imagerie SAR: Application aux modélisations sismo-volcaniques. PhD thesis. Univ Grenoble. France. 2011.
- [26]. Rosen, P-A. Hensley, S. Peltzer, G. and al. Updated repeat orbit interferometry package released. Earth Observation Syst. Trans., Amer. Geophys. Union, Electronic Supplement. 2004. p. 47. Vol. 85.
- [27]. Cavalie, O. Doin, M. Lasserre, C. and al. Ground motion measurement in the lake Mead area, Nevada, by differential synthetic aperture radar interferometry time series analysis: Probing the lithosphere rheological structure. Journal of Geophysical Research. 2007. Vol. 112. B03403.

- [28]. Rosen, P. Persaud, P. ROI_PAC Documentation Repeat Orbit Interferometry Package Version 1.1, Abridged version of Chapter 3 of a PhD thesis written by Sean Buckley CSR, UT Austin. 2000.
- [29]. Biggs, J. Wright, T. Lu, Z. and al. Multi-interferogram method for measuring interseismic deformation: Denali Fault, Alaska. *Geophys. J. Int.* 2007. pp. 1165–1179. Vol. 170.
- [30]. Elliott, J-R. Biggs, J. Parsons, B. and al. InSAR slip rate determination on the AltynTagh Fault, northern Tibet, in the presence of topographically correlated atmospheric delays. *Geophysical Research Letters.* 2008. Vol. 35. L12309.
- [31]. Lundgren, P. Usai, S. Sansosti, E. and al. Modeling surface deformation observed with synthetic aperture radar interferometry at CampiFlegrei caldera .106, 19, 355-19, 366. *Journal of Geophysical Research.* 2001. pp. 355-366. Vol. 106.
- [32]. Berardino, P. Fornaro, G. Lanari, R. and al. A new algorithm for surface deformation monitoring based on small baseline differential SAR interferograms. *IEEE Trans. Geosci Remote Sens.* 2002. pp. 2375–2383. Vol. 40.
- [33]. Mora, O. Mallorqui, J-J. Broquetas, A. Linear and non linear terrain deformation maps from a reduced set of interferometric SAR images. *IEEE Trans Geosci Remote Sens.* 2003. pp. 2243–2253. Vol. 41.
- [34]. Lanari, R. Mora, O. Manunta, M. and al. A small baseline approach for investigating deformations on full resolution differential SAR interferograms. *IEEE Trans Geosci Remote Sens.* 2004. Vol. 42.
- [35]. Lanari, R. Casu, F. Manza, M. and al. Application of the SBAS-DInSAR technique to fault creep: A case study of the Hayward fault, California . *Environ Remote Sens.* 2007. pp. 20-28. Vol. 109.
- [36]. Champenois, J. Caractérisation des déformations tectoniques inter-sismiques de l'île de Taiwan par interférométrie radar. PhD thesis. Univ Paris Est Marne-la-Valée. 2011. pp 37-50.
- [37]. Peltzer, G. Crampe, F. Hensley, S. and al. Transient strain accumulation and fault interaction in the Eastern California shear zone. *Geology.* 2001. pp. 975–978. Vol. 29.
- [38]. Wright, T. Parsons, B. Fielding, E. Measurement of interseismic strain accumulation across the north anatolian fault by satellite radar interferometry. *Geophysical Research Letters.* 2001. pp. 2117–2120. Vol. 28.
- [39]. Zebker, H-A. Rosen, P-A. Hensley, S. Atmospheric effects in interferometric synthetic aperture radar surface deformation and topographic maps. *Journal of Geophysical Research.* 1997. pp. 7547–7563. Vol. 102.
- [40]. Raucoules, D. Maisons, C. Carnec, C. and al. Suivi de subsidence sur le site de la saline de vauvert par Interférométrie radar. Lille 2004 (28 - 30 juin). National days of Geotechnics and Geology of the engineer 2004. pp. 413-417.
- [41]. Hanssen, R-F. Radar interferometry: Data interpretation and error analysis. Kluwer Academic Publishers. 2001. pp. 100-130.
- [42]. Menedez, T-C. Fusion de mesures de déplacement: application à l'estimation du champs de déformation dû à un tremblement de terre. Project of Study End of Engineers. 2008.
- [43]. Médioni, R. Wernli, R. Étude géologique du bassin post nappe miopléocène de Charf El Akab (Province de Tanger). *Notes Mém. Serv. Géol. Maroc.* 1978. p. 276.
- [44]. Humbert, M. Mémoire explicatif de la carte géotechnique de Tanger 1/25 000. *Géologie & Morphologie, Contribution à la connaissance du Tangerois. Notes Mém. Serv. Géol. Maroc.* 1971. pp. 31-33. Vol. 222 bis.
- [45]. Didon, J. Durand-Delga, M. Esteras M. and al. Les formations des grès numidiens de l'arc de Gibraltar s'intercalent stratigraphiquement entre les argiles d'oligocènes et des marnes burdigaliennes. *C.R. Acad. Sci. Paris.* 1984. pp. 121-128. Vol. 3.
- [46]. Hoyez, B. Le Numidien et les flyschs oligo-miocènes de la bordure sud de la Méditerranée occidentale. PhD thesis. Univ Lille. 1989.
- [47]. Achab, M. El Moumni, B. El Arrim, A. and al. Répartition des faciès sédimentaires récents en milieu marin côtier: exemple des baies de Tanger (NW-Maroc) et de Cadix (SW-Espagne). *Bull. Inst Sci. Rabat, sec. Sci. Terre.* 2005. Vol. 27.
- [48]. Ezzouak, F. Etude géotechnique de la ville de Tanger et ses environs. *Géoressources et Milieu Naturel. Univ Abdelmalek Essaadi, Tetouan. Thesis Post-Graduate studies.* 2008. pp. 63-64.
- [49]. El Fahsi, A. Tectonique alpine, néotectonique et étude des formations marines quaternaire de rive sud du Détroit de Gibraltar entre Tanger et Sebta (Rif, Maroc). *D.E.S. Univ Mohammed V - Rabat.* 1999. pp. 200- 230.